
Graph Bernoulli Pooling

Paper Id: 3310

Abstract

1 Graph pooling is crucial for enlarging receptive field and reducing computational
2 cost in deep graph representation learning. In this work, we propose a simple
3 but effective non-deterministic graph pooling method, called graph Bernoulli
4 pooling (BernPool), to facilitate graph feature learning. In contrast to most graph
5 pooling methods with deterministic modes, we design a probabilistic Bernoulli
6 sampling to reach an expected sampling rate through deducing a variational bound
7 as the constraint. To further mine more useful info, a learnable reference set is
8 introduced to encode nodes into a latent expressive probability space. Hereby
9 the resultant Bernoulli sampling would endeavor to capture salient substructures
10 of the graph while possessing much diversity on sampled nodes due to its non-
11 deterministic manner. Considering the complementarity of node dropping and
12 node clustering, further, we propose a hybrid graph pooling paradigm to combine
13 a compact subgraph (via dropping) and a coarsening graph (via clustering), in
14 order to retain both representative substructures and input graph info. Extensive
15 experiments on multiple public graph classification datasets demonstrate that our
16 BernPool is superior to various graph pooling methods, and achieves state-of-
17 the-art performance. The code is publicly available in an anonymous format at
18 <https://github.com/BernPool>.

19 1 Introduction

20 Graph Neural Networks (GNNs) [13, 36] have been widely used to learn expressive representation
21 from ubiquitous graph-structured data such as social networks [31], chemical molecules [15] and
22 biological networks [24]. To improve representation ability, multiple GNN variants, e.g., graph
23 convolutional networks (GCNs) [16] and graph attention networks (GATs) [25], have been developed
24 to facilitate various graph-related tasks including node classification[16], link prediction[19, 35], and
25 graph classification[36]. Specifically, for graph-related learning tasks, graph pooling has become
26 an essential component in various GNN architectures. Aiming to learn compact representation for
27 graphs, graph pooling facilitates graph topology modeling by enlarging receptive fields as well as
28 scaling down the graph size which effectively reduces computational costs.

29 The existing graph pooling techniques generally fall into two main categories, i.e., the global graph
30 pooling [5, 27, 14, 33, 26, 36] and hierarchical graph pooling. The former directly compresses a set
31 of nodes into a compact graph-level representation. This operation results in a flat feature as a whole
32 graph embedding. In contrast, the hierarchical pooling coarsens graphs gradually and outputs the
33 corresponding pooled graphs of smaller sizes. For this purpose, two different types of coarsening,
34 named node dropping [17, 10, 20, 37, 18, 11] and node clustering [33, 1, 34], are often employed.
35 The node dropping picks up a subset of nodes to construct the coarsened graph, while the node
36 clustering learns an assignment matrix to aggregate those nodes in the original graph into new clusters.
37 In this work, our proposed BernPool falls in the category of the latter.

38 Even though considerable progress has been made, most pooling methods select a part of nodes or
39 cluster nodes in a deterministic manner according to the importance scores of nodes, which degrades
40 the sampling diversity. For this issue, some previous works [21, 7] propose stochastic node dropping
41 independent from the data, i.e., randomly dropping. However, they do not consider the intrinsic

42 structural characteristics of data while enriching the sampling diversity. Thus the current bottleneck
43 is how to adaptively extract expressive substructures and meanwhile keeping rich sampling diversity
44 in graph pooling, with the precondition of high-efficient and effective graph representation learning.

45 To address the above problem, in this work, we propose a graph Bernoulli pooling method called
46 BernPool to facilitate graph representation learning. Different from the existing graph pooling
47 methods, we design a probabilistic Bernoulli sampling by estimating the sampling probabilities of
48 graph nodes. To restrict the sampling process, we formulate a variational Bernoulli learning constraint
49 by deriving an upper bound between an expected distribution and a learned distribution. To better
50 capture expressive info, a learnable reference set is further introduced to encode nodes into a latent
51 expressive probability space. Thus the advantage of the resultant Bernoulli sampling is two-fold: i)
52 capture representative substructures of graph; and ii) preserve certain diversity (like random dropping)
53 due to its non-deterministic manner. Considering the complementary characteristics between node
54 dropping and node clustering, we propose a hybrid graph pooling paradigm to fuse a compact
55 subgraph after node dropping and a coarsening graph after node clustering. The node clustering
56 in our framework is also Bernoulli-induced without high-computation cost because it adopts the
57 sampled nodes as clustering centers. The hybrid graph pooling can jointly learn representative
58 substructures and preserve the input graph topology. We conduct extensive experiments on 8 public
59 graph classification datasets to test our BernPool, and the experimental results validate that our
60 BernPool achieves better performance than those existing pooling methods and keep high efficiency
61 on par with those node-dropping methods.

62 The contributions of this work are summarized as: i) propose a probabilistic Bernoulli sampling
63 method to not only learn effective sampling but also preserve high efficiency; ii) propose a hybrid
64 graph pooling way to retain both those sampled substructures and the remaining info; iii) verify the
65 effectiveness and high-efficiency of our BernPool, and report the state-of-the-art performance.

66 2 Related Work

67 In this section, we first review the previous methods of Graph Neural Networks (GNNs), then
68 introduce the related Hierarchical pooling methods.

69 **Graph Neural Network.** GNNs were introduced as a form of recurrent neural network by Gori
70 et.al. [12] and Scarselli et al. [23]. Subsequently, Duvenaud et al.[6] introduced a convolution-
71 like propagation rule on graphs to extract node representations for graph-level classification. To
72 enhance the graph representation ability, several convolution operations were proposed (e.g. Graph
73 Convolution Network(GCN[16]), Graph Attention Network(GAT[25]), GraphSAGE[13], GIN[30])
74 to extract expressive node representations by aggregating neighbor node features and have achieved
75 promising performance in various graph-related tasks in recent years. In particular, GCN[16] utilizes
76 a first-order approximation of spectral convolution via Chebyshev polynomial iteration to improve
77 efficiency. However, it suffers from the issue of fixed and equal weighting for neighbor nodes during
78 aggregation, which may not be optimal for all nodes and can lead to information loss. To address this
79 problem, GAT[25] introduced an attention mechanism to assign different weights to neighbor nodes
80 during message passing. Furthermore, GrapSAGE[13] learned node embeddings by aggregating
81 feature information from the neighborhood in an inductive manner. Despite the considerable progress
82 made by GNNs, they are limited in their ability to generate hierarchical graph representations due to
83 the lack of pooling operations.

84 **Hierarchical Graph Pooling.** Graph pooling is a critical operation to obtain robust representations
85 and scale down the size of graphs, which can be classified into two categories: global pooling
86 and hierarchical pooling. The former [5, 27, 14, 33, 26, 36] aggregates node-level features to
87 generate a graph-level representation. For instance, SortPool[36] ranks and groups the nodes into
88 clusters according to their features, then aggregates the resulting clusters to generate the graph-
89 level representation. However, the global pooling suffers from the issue of discarding structure
90 information in generating graph-level representation. On the other hand, the hierarchical pooling
91 methods could progressively compress the graph into a smaller one and capture the hierarchical
92 structure. They can be further divided into node clustering pooling methods [33, 1, 34], node drop
93 pooling methods [17, 10, 20, 37, 18, 11] and other pooling methods[28, 3]. Among them, the
94 node drop pooling methods deleted the unimportant nodes based on certain criteria. For instance,
95 SAGPool [17] computed the node attention scores using graph convolution to preserve the most

96 important nodes. But the node drop pooling methods may not preserve the original structure well
 97 during the graph compression process. To alleviate this problem, Pang et.al [20] applied contrastive
 98 learning to maximize the mutual information between the input graph and the pooled graphs to
 99 preserve the graph-level dependencies in the pooling layers. Gao et.al [11] proposed a criterion to
 100 assess each node’s information among its neighbors to retain informative features. Our BernPool
 101 introduces probabilistic deduced Bernoulli sampling based on reference set to progressively compress
 102 the original graph by preserving important nodes, rather than selecting nodes in a deterministic
 103 way. This probabilistic manner can lead to more diverse sampling situations and capture the data of
 104 intrinsic characteristics, promoting graph discriminative representation learning. Furthermore, we
 105 propose a hybrid graph pooling module to alleviate the node drop pooling method’s issue of cannot
 106 preserve structure well.

107 3 Preliminaries

108 **Notations** For an arbitrary graph $\mathcal{G} = (\mathcal{V}, \mathcal{E}, \mathbf{X})$ with $n = |\mathcal{V}|$ nodes and $|\mathcal{E}|$ edges. $\mathbf{X} \in \mathbb{R}^{n \times d'}$
 109 represents the node feature matrix, where d' is the dimension of node attributes, and $\mathbf{A} \in \mathbb{R}^{n \times n}$
 110 denotes the adjacency matrix describing its edge connection information. The graph \mathcal{G} has a one-hot
 111 vector \mathbf{y}_i w.r.t its label. A pooled graph of the original graph \mathcal{G} is denoted by $\tilde{\mathcal{G}} = (\tilde{\mathcal{V}}, \tilde{\mathcal{E}}, \tilde{\mathbf{X}})$ with
 112 adjacency matrix as $\tilde{\mathbf{A}} \in \mathbb{R}^{\tilde{n} \times \tilde{n}}$, where \tilde{n} denotes the number of pooled nodes.

113 **Graph Convolution** In this work, we employ the classic graph convolution network (GCN) as the
 114 backbone to extract features, where the l -th convolutional layer is formulated as:

$$\mathbf{H}^{(l+1)} = \sigma(\hat{\mathbf{D}}^{-\frac{1}{2}} \hat{\mathbf{A}} \hat{\mathbf{D}}^{\frac{1}{2}} \mathbf{H}^{(l)} \mathbf{W}^{(l)}), \quad (1)$$

115 where $\sigma(\cdot)$ is a non-linear activation function, $\mathbf{H}^{(l)}$ is the hidden-layer feature, $\hat{\mathbf{A}}$ is the added
 116 self-loop adjacent matrix, $\hat{\mathbf{D}}$ denotes the degree matrix of $\hat{\mathbf{A}}$, and $\mathbf{W}^{(l)}$ represents a learnable weight
 117 matrix at the l -th layer. The initial node features are used at the first convolution, i.e., $\mathbf{H}^{(0)} = \mathbf{X}$.

118 4 The Proposed BernPool

119 4.1 Overview

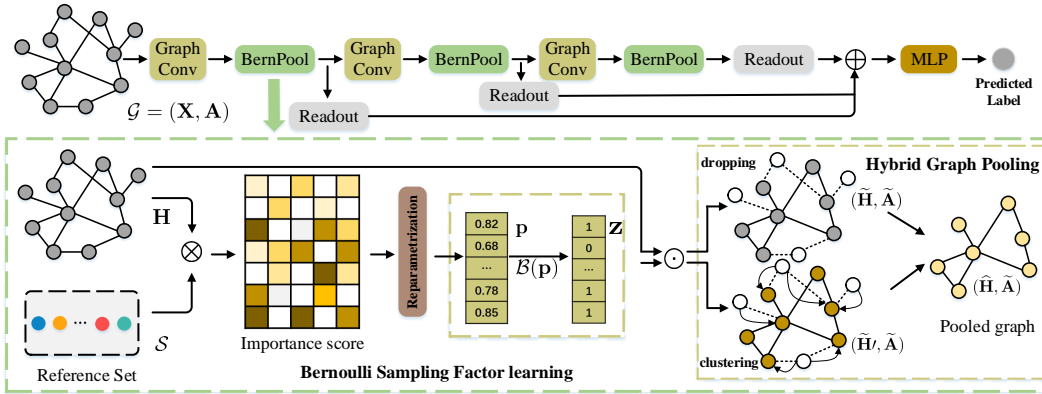


Figure 1: The architecture of the proposed BernPool framework. Please see Overview in Section 4.1.

120 The whole framework is illustrated in Fig. 1, where the convolution and our proposed BernPool are
 121 stacked alternately. The proposed BernPool could be seamlessly engaged with any type of graph
 122 convolution to facilitate graph representation. In BernPool, there contains two main modules: graph
 123 Bernoulli sampling (GBS) and hybrid graph pooling (HGP). To boost graph Bernoulli sampling,
 124 we specifically design a reference set \mathcal{S} to encode the importance of each graph node, and the
 125 reference set is configured as the optimizable parameters. The reference set is further conditioned on
 126 the orthogonal space so as to reduce redundancy. After transforming via the reference set, we can

127 estimate the sampling probabilities \mathbf{p} of graph nodes. In particular, the probabilities of nodes are
 128 totally restricted with an expected/predefined distribution, which is formulated to maximize the upper
 129 bound of KL-divergence (please see Section 4.2). Just due to the restriction, we can probabilistically
 130 sample a specified proportion of graph nodes. The detail of GBS can be found in Section 4.3. In the
 131 stage of hybrid graph pooling, on the one hand, we prune those unsampled nodes and the associated
 132 edges to generate a compact subgraph; on the other hand, to preserve graph topological structure,
 133 we perform neighbor nodes clustering to form a coarsening graph. Both the compact subgraph
 134 and coarsening graph are fused to form the final pooled graph. The detail of HGP can be found in
 135 Section 4.4. The BernPool attempts to learn the reference set and a few linear transformations. The
 136 whole framework can be optimized in an end-to-end mode through back-propagation.

137 4.2 Bernoulli Sampling Optimization Objective

138 To sample a certain proportion of graph nodes in a probabilistic manner, we derive a KL-divergence
 139 constraint, which makes node probabilities tend to be a predefined distribution. To this end, we again
 140 dissect mutual information between the learned subgraph embeddings and their corresponding labels.
 141 Formally, we aim to maximize the mutual information function:

$$\zeta_{MI} = MI(\mathbf{y}, f_{\psi, \phi}(\mathcal{G}, \mathcal{S})), \quad (2)$$

142 where ϕ denotes the parameters of the BernPool, ψ is the parameters of other modules (e.g., convolu-
 143 tion, classifier), and $f_{\psi, \phi}(\cdot)$ represents the graph embedding process.

144 Suppose the sampling factor \mathbf{z} in graph pooling, we resort to the relationship between mutual
 145 information and expectation, and rewrite Eqn. (2) as:

$$\begin{aligned} & \mathbb{E}_{\mathbf{y}|\mathcal{G}, \mathcal{S}}[\log \int p_{\psi}(\mathbf{y}|\mathcal{G}, \mathcal{S}, \mathbf{z})p_{\phi}(\mathbf{z}|\mathcal{G}, \mathcal{S})d\mathbf{z}] \\ &= \mathbb{E}_{\mathbf{y}|\mathcal{G}, \mathcal{S}}[\log \int q_{\phi}(\mathbf{z}|\mathcal{G}, \mathcal{S})p_{\psi}(\mathbf{y}|\mathcal{G}, \mathcal{S}, \mathbf{z})\frac{p_{\phi}(\mathbf{z}|\mathcal{G}, \mathcal{S})}{q_{\phi}(\mathbf{z}|\mathcal{G}, \mathcal{S})}d\mathbf{z}], \end{aligned} \quad (3)$$

146 where $p_{\psi}(\mathbf{y}|\mathcal{G}, \mathcal{S}, \mathbf{z})$ is the conditional probability of label \mathbf{y} , and $p_{\phi}(\mathbf{z}|\mathcal{G}, \mathcal{S})$ denotes the conditional
 147 probability of the factor \mathbf{z} that is usually intractable. After a series of derivation from Eqn. (3), we
 148 can deduce a bound with KL-divergence between expected Bernoulli distribution q_{ϕ} and learned
 149 distribution p_{ϕ} :

$$\begin{aligned} & \mathbb{E}_{\mathbf{y}|\mathcal{G}, \mathcal{S}}[\log \int p_{\psi}(\mathbf{y}|\mathcal{G}, \mathcal{S}, \mathbf{z})p_{\phi}(\mathbf{z}|\mathcal{G}, \mathcal{S})d\mathbf{z}] \\ & \geq \mathbb{E}_{\mathbf{y}|\mathcal{G}, \mathcal{S}}[\log p_{\psi}(\mathbf{y}|\mathcal{G}, \mathcal{S}, \mathbf{z})] - D_{KL}(q_{\phi}(\mathbf{z}|\mathcal{G}, \mathcal{S})||p_{\phi}(\mathbf{z}|\mathcal{G}, \mathcal{S})) \end{aligned} \quad (4)$$

$$= -\zeta_{CE} - D_{KL}(q_{\phi}(\mathbf{z}|\mathcal{G}, \mathcal{S})||p_{\phi}(\mathbf{z}|\mathcal{G}, \mathcal{S})), \quad (5)$$

150 where $p_{\psi}(\mathbf{y}|\mathcal{G}, \mathcal{S})$ represents the predicted probability of label based on the input graph and reference
 151 set. ζ_{CE} is the cross entropy loss function. **Please see the detailed derivation in the supplementary**
 152 **file.** As the expected Bernoulli distribution $q_{\phi}(\mathbf{z}|\mathcal{G}, \mathcal{S})$ is independent from the input graph and
 153 reference set, $q_{\phi}(\mathbf{z}|\mathcal{G}, \mathcal{S})$ can be denoted as $q(\mathbf{z})$. After adding the soft-orthogonal constraint on the
 154 reference set, therefore, the final optimization objective can be converted to minimize:

$$\zeta = \zeta_{CE} + D_{KL}(q(\mathbf{z})||p_{\phi}(\mathbf{z}|\mathcal{G}, \mathcal{S})) + \beta\|\mathbf{S}\mathbf{S}^{\top} - c\mathbf{I}\|_F, \quad (6)$$

155 where the second term forces the sampling factor to follow an expected distribution q , the matrix \mathbf{S}
 156 stacks the vectors of reference set \mathcal{S} in the third term, \mathbf{I} denotes the identity matrix, β is a trade-off
 157 hyper-parameter, and c is a learnable scalar. Thus, the learning of the sampling factor could be
 158 integrated into the objective function as a joint training process. In addition, we can easily extend the
 159 above single-layer BernPool into multi-layer networks by deploying independent sampling factors in
 160 sequential graph pooling.

161 4.3 Bernoulli Sampling Factor Learning

162 To extract an expressive sub-graph $\tilde{\mathcal{G}}$ from the original or former-layer graph \mathcal{G} , we estimate a
 163 probabilistic factor $\mathbf{z} = (z_1, \dots, z_n)^{\top} \in \{0, 1\}^n$ that conforms to Bernoulli distribution, instead
 164 of a deterministic way such as top-k. In contrast to the deterministic way, our BernPool possesses

165 a more diverse sampling in mining substructures and graph topological variation of input data.
 166 However, as mentioned above in Eqn. (3), it’s rather non-trivial to infer \mathbf{z} through Bayes rule:
 167 $p(\mathbf{z}|\mathcal{G}, \mathcal{S}) = p(\mathbf{z})p(\mathcal{G}, \mathcal{S}|\mathbf{z})/p(\mathcal{G}, \mathcal{S})$. A reason is that the prior $p(\mathcal{G}, \mathcal{S}|\mathbf{z})$ is intractable. We resort
 168 to the variational inference to approximate the intractable true posterior $p(\mathbf{z}|\mathcal{G}, \mathcal{S})$ with $q(\mathbf{z})$ by
 169 constraining the KL-divergence $D_{KL}(q_\phi(\mathbf{z})||p_\phi(\mathbf{z}|\mathcal{G}, \mathcal{S}))$.

170 To make the gradient computable, we employ the reparameterization trick to derive $p(\mathbf{z}|\mathcal{G}, \mathcal{S}) = \mathcal{B}(\mathbf{p})$,
 171 where $\mathcal{B}(\cdot)$ denotes the Bernoulli distribution based on the probability vector. Concretely, we take
 172 the graph convolution feature \mathbf{H} and the matrix \mathbf{S} of reference set as input, to learn the sampling
 173 probability \mathbf{p} . A simple formulation with a fully-connected operation is given as follows:

$$\mathbf{p} = \text{sigmoid}(\text{MLP}(\cos(\mathbf{H}, \mathbf{S}))), \quad (7)$$

174 where $\cos(\mathbf{H}, \mathbf{S})$ computes the pairwise similarities (across all graph nodes and all reference points)
 175 through the cosine measurement, and $\text{sigmoid}(\cdot)$ is the sigmoid function.

176 4.4 Bernoulli Hybrid Graph Pooling

177 Based on the above inferred sampling factor \mathbf{z} , we propose a hybrid graph pooling to learn expressive
 178 substructures while endeavoring to reserve graph information. The hybrid graph pooling contains
 179 two components: Bernoulli node dropping and Bernoulli node clustering. The former prunes those
 180 unsampled nodes and associated edges to generate a compact graph; the latter clusters neighbor nodes
 181 to form a coarsening graph.

182 **Bernoulli Node Dropping.** Let $\text{idx} \in \mathbb{R}^{\tilde{n}}$ denotes the indices of the preserved nodes according to the
 183 sampling factor \mathbf{z} , thus a projection matrix $\mathbf{P} \in \{0, 1\}^{\tilde{n} \times n}$ can be defined formally:

$$\mathbf{P} = \text{diag}(\mathbf{z})[\text{idx}, :], \quad (8)$$

184 where $\text{diag}(\cdot)$ is the vector diagonalization operation, and $\mathbf{X}[\text{idx}, :]$ extracts those rows of \mathbf{X} w.r.t the
 185 indices idx . Accordingly, the compact subgraph $\tilde{\mathcal{G}} = (\tilde{\mathbf{H}}, \tilde{\mathbf{A}})$ can then be computed by:

$$\tilde{\mathbf{H}} = \mathbf{P}\mathbf{H}, \quad \tilde{\mathbf{A}} = \mathbf{P}\mathbf{A}\mathbf{P}^\top, \quad (9)$$

186 where $\tilde{\mathbf{H}} \in \mathbb{R}^{\tilde{n} \times d}$ is the feature matrix of the compact graph, and $\tilde{\mathbf{A}} \in \mathbb{R}^{\tilde{n} \times \tilde{n}}$ is the subgraph
 187 adjacency matrix. Intuitively, the dropping directly removes those unselected nodes and connective
 188 edges from the input graph.

189 **Bernoulli Node Clustering.** After Bernoulli sampling, we can obtain those reserved nodes, which
 190 could be used as the clustering centers. Hereby, we only need to transmit those unselected nodes’
 191 messages to cluster centers, which would preserve more information of the whole input graph.
 192 Compared with previous graph clustering methods, Bernoulli clustering is more efficient because the
 193 learning of the assignment matrix is bypassed, while increasing the diversity of graph perception. To
 194 be specific, our assignment matrix $\mathbf{P}' \in \mathbb{R}^{\tilde{n} \times n}$ is from the original adjacency matrix \mathbf{A} , and we can
 195 get the coarsening graph as:

$$\mathbf{P}' = (\text{diag}(\mathbf{z})[\text{idx}, :]) \times \mathbf{A}, \quad \tilde{\mathbf{H}}' = \mathbf{P}'\mathbf{H}, \quad (10)$$

196 where $\tilde{\mathbf{H}}' \in \mathbb{R}^{\tilde{n} \times d}$ denotes the diffusion features based on input graph, the coarsening graph has the
 197 same adjacency matrix $\tilde{\mathbf{A}}_i$ as in Eqn. (9).

198 **Hybrid Graph.** Based on the aforementioned operations, we can obtain the compact subgraph
 199 $\tilde{\mathcal{G}} = (\tilde{\mathbf{H}}, \tilde{\mathbf{A}})$ and the coarsening graph $\tilde{\mathcal{G}}' = (\tilde{\mathbf{H}}', \tilde{\mathbf{A}})$, which reflect different aspects of information in
 200 the original graph. To fully exploit the extracted informative node representations and expressive sub-
 201 structures, the two subgraphs are fused to form the final pooled graph by the following formulation:

$$\hat{\mathbf{H}} = \sigma((\tilde{\mathbf{H}} + \tilde{\mathbf{H}}')\mathbf{W}_h), \quad (11)$$

202 where σ denotes a non-linear activation function and $\mathbf{W}_h \in \mathbb{R}^{d \times d}$ is a learnable weight, and
 203 $\hat{\mathbf{H}} \in \mathbb{R}^{\tilde{n} \times d}$ is the aggregated node embeddings of the pooled graph.

204 **4.5 Readout Function**

205 The proposed framework repeats the graph convolution and BernPool operations three times. To
206 obtain a fixed-size graph-level representation, we apply the concatenation of max-pooling and mean-
207 pooling in each subgraph following the previous works [37, 29, 22]. Finally, those graph-level
208 representations can be summarized to form the final embeddings:

$$\mathbf{r} = \sum_{l=1, \dots} \mathbf{r}^{(l)}, \quad \text{and} \quad \mathbf{r}^{(l)} = \sigma\left(\frac{1}{n_i^{(l)}} \sum_{i=1}^{n_i^{(l)}} \widehat{\mathbf{H}}_i^{(l)} \parallel \max_{i=1}^{n_i^{(l)}} \widehat{\mathbf{H}}_i^{(l)}\right), \quad (12)$$

209 where $\widehat{\mathbf{H}}_i^{(l)}$ denotes the i -th node feature at the l -th pooling, σ is the same non-linear activation
210 function, and \parallel denotes the feature concatenation operation. The resulting embeddings would finally
211 be fed into a multi-layer perceptron to predict graph labels.

212 **4.6 Computational Complexity**

213 The computational complexity of one-layer BernPool can be expressed as $O(N \times K \times d + N' \times N \times$
214 $d + N' \times d \times d)$, where N denotes the number of nodes, K is the number of reference points, d is
215 the dimensionality of nodes features, N' represents the number of preserved nodes. Specifically, the
216 complexity of probability score computation is $O(N \times K \times d)$, and the complexity of the Bernoulli
217 hybrid graph pooling module is $O(N' \times N \times d + N' \times d \times d)$.

218 **5 Experiments**

219 **5.1 Experimental Setup**

220 **Datasets.** To comprehensively evaluate our proposed model, we conduct extensive experiments
221 on eight widely used datasets in the graph classification task, including three social network
222 datasets (IMDB-BINARY, IMDB-MULTI [31] and COLLAB[32]) and five Bioinformatics datasets
223 (PROTEINS[8], DD[4], NCI1[24], Mutagenicity[15] and ENZYMES[2]). The detailed information
224 and statistics of these datasets are summarized in Table. 1.

225 **Baselines.** We compare our proposed method with several state-of-the-art graph pooling methods,
226 including three backbones (GCN, GAT, GraphSAGE), eight node drop graph pooling methods
227 (TopkPool[10], SAGPool[17], ASAP[22], VIPool[18], iPool[11], CGIPool[20], SEP-G [29] and
228 MVPool [37]), three clustering pooling methods (Diffpool[33], MincutPool[1], and StructPool[34]),
229 three global pooling methods (Set2Set[26], SortPool[36], DropGIN[21]) and one other pooling
230 method (EdgePool[3]).

231 **Implementation Details.** We employ the 10-fold cross-validation protocol following the settings of
232 [29, 22] and report the average classification accuracies and standard deviation. For all used datasets,
233 we set the expected pooling ratio as 0.8, the node embedding dimension d as 128, the number of
234 reference points as 32, and the hyper-parameter β in Eqn. 6 as 5. We adopt the Adam optimizer to
235 train our model with 1000 epochs, where the learning rate and weight decay are set as 1e-3 and 1e-4,
236 respectively. Our proposed BernPool is implemented with PyTorch and Pytorch Geometric [9].

237 **5.2 Comparison with the state-of-the-art Methods**

238 The graph classification results of BernPool and other state-of-the-art methods are presented in Table 1.
239 In general, most hierarchical pooling approaches including our proposed BernPool can perform better
240 than those global pooling ones in the graph classification task. This may be because global pooling
241 methods ignore the hierarchical graph structures in generating graph-level representation. In particular,
242 our BernPool achieves state-of-the-art performance on all datasets, which demonstrates the robustness
243 of our framework against graph structure data variation. In contrast, previous methods cannot perform
244 well on all eight datasets, while the second highest performances on different datasets are obtained
245 by five different methods. Compared with those methods, Our BernPool outperforms respectively
246 by 1.09%, 3.16%, 13.6%, 2.7%, and 1.86% on the PROTEINS, Mutagenicity, ENZYMES, IMDB-
247 BINARY and COLLAB datasets.

Table 1: **The statistics of eight datasets and graph classification accuracies comparison of different methods.** We have highlighted the best results in black and marked the second-highest accuracies with the symbol †.

	Bioinformatics					Social Network		
	PROTEINS	DD	NCI1	Mutagenicity	ENZYMES	IMDB-B	IMDB-M	COLLAB
#Graphs(Classess)	1113 (2)	1178 (2)	4110 (2)	4337 (2)	600 (6)	1000 (2)	1500 (3)	5000 (3)
Avg # Nodes	39.1	284.3	29.8	30.3	32.6	19.8	13.0	74.5
Avg # Edges	72.8	715.7	32.3	30.8	62.1	96.5	65.9	2457.8
GCN[16]	74.84±2.82	78.12±4.33	76.3±1.8	79.8±1.6	50.00±5.87	72.67±6.42	50.40±3.02	71.92±3.24
GAT[25]	74.07±4.53	75.56±3.72	74.9±1.7	78.8±1.2	51.00±5.23	74.07±4.53	49.67±4.30	75.80±1.60
GraphSAGE[13]	73.75±2.97	77.27±4.06	74.7±1.3	78.9±2.1	53.33±3.42	72.17±5.29	48.53±5.43	79.70±1.70
Set2Set[26]	73.27±0.85	71.94±0.56	68.55±1.92	71.35±2.1	-	72.90±0.75	50.19±0.39	79.55±0.39
SortPool[36]	73.27±0.85	75.58±0.72	73.82±1.96	70.66±1.51	49.67±4.27	72.12±1.12	48.18±0.83	77.87±0.47
DropGIN[21]	76.3±6.1	-	-	-	-	75.7±4.2	51.4±2.8	-
EdgePool[3]	72.50±3.2	75.85±0.58	-	-	-	72.46±0.74	50.79±0.59	67.10±2.7
DiffPool[33]	73.03±1.00	77.56±0.41	62.32±1.90	77.60±2.70	61.83±5.3	73.14±0.70	51.31±0.72	78.68±0.43
StructPool[34]	80.36	84.19	-	-	63.83	74.70	52.47	74.22
MinCutPool[1]	76.5±2.6	80.8±2.3	74.25±0.86	79.9±2.1	-	72.65±0.75	51.04±0.70	83.4±1.7†
TopKPool[10]	70.48±1.01	73.63±0.55	67.02±2.25	79.14±0.76	50.33±6.3	71.58±0.95	48.59±0.72	77.58±0.85
SAGPool[17]	71.86±0.97	76.45±0.97	67.45±1.11	72.40±2.40	52.67±5.8	72.55±1.28	50.23±0.44	78.03±0.31
ASAP[22]	74.19±0.79	76.87±0.70	71.48±0.42	80.12±0.88	-	72.81±0.50	50.78±0.75	78.64±0.50
VIPool[18]	79.91±4.1	82.68±4.1†	-	80.19±1.02	57.50±6.1	78.60±2.3†	55.20±2.5†	78.82±1.4
iPool[11]	76.46±3.22	78.76±3.45	80.46±1.66†	-	56.00±7.72	72.90±3.08	50.73±3.68	76.86±1.67
SEP-G[29]	76.42±0.39	77.98±0.57	78.35±0.33	-	-	74.12±0.56	51.53±0.65	81.28±0.15
CGIPool[20]	74.10±2.31	-	78.62±1.04	80.65±0.79†	-	72.40±0.87	51.45±0.65	80.30±0.69
MVPool[37]	82.2±1.2†	78.4±1.5	77.5±1.3	80.2±0.8	62.4±2.5†	-	48.6±1.0	-
BernPool(Ours)	83.29 ± 3.69	83.27 ± 2.95	81.44 ± 1.09	83.81 ± 1.43	76.00 ± 3.78	81.30 ± 3.50	55.93 ± 3.8	85.26 ± 1.35

248 Moreover, the proposed BernPool significantly surpasses GNNs (GCN, GAT, GraphSAGE) without
249 adding the pooling operation, which verifies our BernPool can effectively learn representative
250 substructures and preserve graph topological information. SEP-G [29] gains better performance
251 compared with other node drop pooling methods, which utilizes the structural entropy to assess the
252 importance of each graph node. However, our BernPool exhibits an average 5% relative improvement
253 over SEP-G. This can be attributed to our method of learning sampling factors in a probabilistic
254 manner, which possesses more diversity in mining expressive sub-structures compared with the
255 deterministic way. Compared to DiffPool [33], our BernPool outperforms it on all used datasets,
256 verifying the effectiveness of our proposed hybrid graph pooling module, which jointly leverages the
257 advantages of both node drop and clustering methods. Particularly, DropGIN [21] randomly drops
258 nodes in the training process, which is also a probabilistic manner. Our BernPool outperforms it by
259 6.99%, 5.6%, and 4.53% on the PROTEINS, IMDB-BINARY, and IMDB-MULTI datasets. This is
260 because our BernPool considers the characteristics of data and can adaptively handle the topology
261 variations.

262 6 Ablation Study

263 **Effectiveness of the proposed BernPool using GCN variants.** To evaluate the performance of
264 our method by employing different convolution layers, we integrate three widely used ones (i.e.,
265 GCN[16], GAT[25] and GraphSAGE[13]) into our BernPool framework. The results on eight datasets
266 are shown in Table 2. It can be observed that all three variants (BernPool-GCN, BernPool-GAT,
267 BernPool-GraphSAGE) outperform their corresponding backbones, significantly improving the graph
268 classification performances. This observation validates the effectiveness of the proposed BernPool.

269 **Effectiveness of Bernoulli hybrid graph pooling.** To verify the effectiveness of our proposed
270 Bernoulli hybrid graph pooling, we further conduct experiments on eight datasets. As the hybrid graph
271 pooling consists of node dropping and clustering. We separately remove one of the channels and keep
272 the other parts the same. We name the BernPool without dropping and clustering as "BernPool w/o
273 Dropping" and "BernPool w/o Clustering", respectively. The detailed results are reported in Table 3.

Table 2: **Graph classification accuracies of BernPool using different backbones.** The default backbone is GCN.

Variants	Bioinformatics					Social Network		
	PROTEINS	DD	NCII	Mutagenicity	ENZYMES	IMDB-B	IMDB-M	COLLAB
#Graphs(Classess)	1113 (2)	1178 (2)	4110 (2)	4337 (2)	600 (6)	1000 (2)	1500 (3)	5000 (3)
GCN	74.84±2.82	78.12±4.33	76.3±1.8	79.8±1.6	50.00±5.87	72.67±6.42	50.40±3.02	71.92±3.24
BernPool-GCN	83.29±3.69 ↑	83.27±2.95 ↑	81.44±1.09 ↑	83.81±1.43 ↑	76.00±3.78 ↑	81.30±3.5 ↑	55.93±3.8 ↑	85.26±1.35 ↑
GAT	74.07±4.53	75.56±3.72	74.9±1.7	78.8±1.2	51.00±5.23	74.07±4.53	49.67±4.30	75.80±1.60
BernPool-GAT	81.49±3.81 ↑	83.44±3.57 ↑	81.29±1.77 ↑	84.34±1.58 ↑	69.50±5.45 ↑	81.20±3.39 ↑	55.00±4.47 ↑	83.86±1.57 ↑
GraphSAGE	73.75±2.97	77.27±4.06	74.7±1.3	78.9±2.1	53.33±3.42	72.17±5.29	48.53±5.43	79.70±1.70
BernPool-GraphSAGE	83.20±4.21 ↑	82.25±3.49 ↑	82.34±1.61 ↑	84.67±1.26 ↑	75.67±3.78 ↑	81.60±3.60 ↑	55.47±3.87 ↑	84.56±1.02 ↑

Table 3: **Performance Comparison between BernPool and its variants.**

Variants	Bioinformatics					Social Network		
	PROTEINS	DD	NCII	Mutagenicity	ENZYMES	IMDB-B	IMDB-M	COLLAB
#Graphs(Classess)	1113 (2)	1178 (2)	4110 (2)	4337 (2)	600 (6)	1000 (2)	1500 (3)	5000 (3)
BernPool w/o Clustering	81.94±4.27	81.66±2.82	78.22±7.69	82.57±1.44	73.00±3.67	80.60±3.13	55.80±4.11	84.52±1.14
BernPool w/o Dropping	82.40±4.02	82.08±3.98	76.20±10.24	82.75±1.44	72.50±4.25	81.30±3.23	55.60±4.16	85.06±1.18
BernPool	83.29±3.69	83.27 ± 2.95	81.44 ± 1.09	83.81 ± 1.43	76.00 ± 3.78	81.30 ± 3.5	55.93 ± 3.8	85.26 ± 1.35

Table 4: **Performance comparison between deterministic and probabilistic manner.**

Variants	Bioinformatics					Social Network		
	PROTEINS	DD	NCII	Mutagenicity	ENZYMES	IMDB-B	IMDB-M	COLLAB
#Graphs(Classess)	1113 (2)	1178 (2)	4110 (2)	4337 (2)	600 (6)	1000 (2)	1500 (3)	5000 (3)
BernPool-TopK	81.77±3.53	82.09±3.25	81.09±1.77	83.26±1.08	68.17±3.72	80.20±3.74	55.47±3.51	84.50±1.40
BernPool	83.29±3.69	83.27 ± 2.95	81.44 ± 1.09	83.81 ± 1.43	76.00 ± 3.78	81.30 ± 3.5	55.93 ± 3.8	85.26 ± 1.35

274 Notably, our BernPool employs just one channel can achieve good results, which demonstrates the
 275 effectiveness of BernPool leveraging a probabilistic manner to infer sampling factors. We can observe
 276 that the "BernPool w/o Dropping" outperforms "BernPool w/o Clustering" by 0.46%, 0.42%, 0.70%,
 277 and 0.54% on PROTEINS, DD, IMDB-BINARY, and COLLAB datasets, respectively. Furthermore,
 278 jointly using both channels can outperform either "BernPool w/o Dropping" or "BernPool w/o
 279 Clustering", which verifies the effectiveness of our proposed hybrid graph pooling.

280 **Comparison between the probabilistic and deterministic manner.** To make clear the benefit
 281 of our proposed probabilistic sampling method, we conduct experiments by replacing Bernoulli
 282 sampling with Topk pooling which is in a deterministic manner. In the TopK experiments, we still
 283 employ reference set to assess the importance of nodes and the hybrid graph pooling module to jointly
 284 learn representative sub-structures and preserve graph topological information. The comparison
 285 between "BernPool-TopK" and "BernPool" is presented in Table 4. It can be observed that BernPool
 286 outperforms BernPool-TopK on all used eight datasets, especially 7.83% accuracy gains in the
 287 ENZYMES dataset, verifying the effectiveness of our designed Bernoulli-deduced sampling strategy.

288 **Benefit of the orthogonality for reference set.** To evaluate the benefit of orthogonality for the
 289 reference set, we conduct experiments that remove the orthogonal constraint from BernPool (referred
 290 to as "BernPool w/o orthogonal" in Fig. 2(a)). The results demonstrate that employing the orthogonal
 291 reference set can improve average accuracy by more than 0.6% on three datasets. This verifies the
 292 effectiveness of the orthogonal constraint for the reference set.

293 **Model parameter quantity comparison.** We compare the test accuracy and parameter quantity
 294 (only the pooling layer) of BernPool with other pooling methods in the PROTEINS dataset, where
 295 the hidden layer dimension is set to 128. BernPool achieves superior performance while using
 296 fewer parameters. Specifically, BernPool owns 97% fewer parameters than CGIPool and 76% fewer
 297 parameters than ASAP. In terms of accuracy, BernPool performs the best, achieving 9.19% higher
 298 than CGIPool and 9.10% higher accuracy than ASAP.

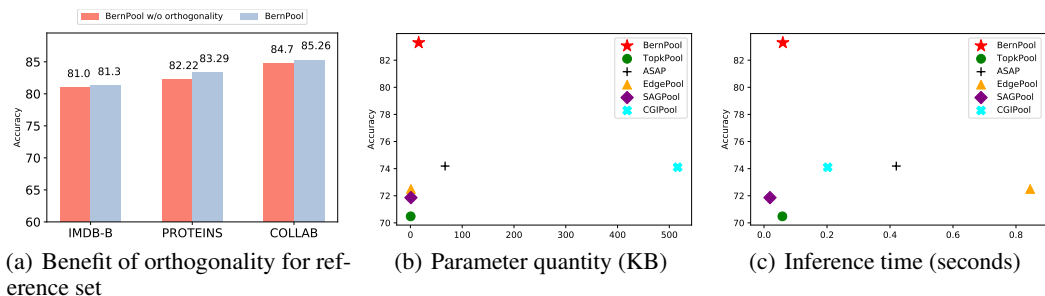


Figure 2: The benefit of orthogonality reference set and comparison of parameter quantity and inference time.

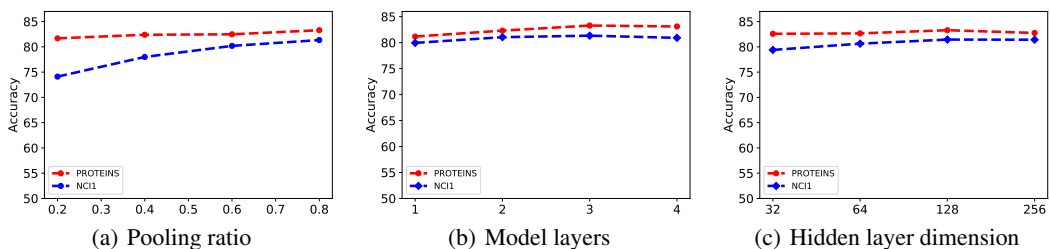


Figure 3: The performance of different hyper-parameters on PROTEINS and NCI1 datasets.

299 **Inference time comparison.** The computation complexity of our BernPool is described in Section 4.6.
 300 Moreover, the inference time also plays a crucial role in evaluating the efficiency of pooling methods.
 301 Thus we conduct experiments on the PROTEINS dataset containing about 20,000 nodes and 70,000
 302 edges to compare the inference time (single-layer). As shown in Fig. 2(c), BernPool costs less
 303 inference time than EdgePool and ASAP while maintaining superior performance. Notably, SAGPool
 304 has a similar inference time as our method, but our method outperforms it in terms of classification
 305 accuracy. The comparison results verify the high efficiency of our BernPool.

306 **Sensitivity of Hyper-parameters.** To evaluate the sensitivity of hyper-parameters, including the
 307 pooling ratio, layer number, and hidden layer dimension, we additionally conduct experiments on
 308 PROTEINS and NCI1 datasets. Specifically, we vary the pooling ratio from 0.2 to 0.8 with a step
 309 length of 0.2, the number of layers from one to four, and the hidden layer dimensions range from 16
 310 to 128. The results are presented in Fig. 3. We can observe that BernPool overall exhibits robustness
 311 to variations of parameters. However, performance fluctuations can be observed on the NCI1 dataset
 312 when we evaluate the effect of different pooling ratios for BernPool. This may be attributed to the
 313 relatively less average number of nodes resulting in less information being retained after performing
 314 three pooling layers consecutively. The results shown in Fig. 3(b) indicate that setting the layer
 315 number to three achieves the best performance on the PROTEINS and NCI1 datasets. However,
 316 increasing the number of layers will require more computation resources and longer training time. As
 317 shown in Fig. 3(c), the highest accuracy is achieved when the dimension size is set as 128. With the
 318 dimension increasing, the accuracy presents a slight increase trend, which suggests that increasing
 319 the dimension size can enhance the model’s capacity to capture more complex representations of the
 320 input graph. However, larger dimension sizes increase computation burdens. Thus we set the pooling
 321 ratio as 0.8, the layer number as 3, and the dimension as 128 in our framework.

322 7 Conclusion

323 In this paper, we proposed a simple and effective graph pooling method, called Graph Bernoulli
 324 Pooling (BernPool) to promote the graph classification task. Specifically, a probabilistic Bernoulli
 325 sampling was designed to estimate the sampling probabilities of graph nodes, and to further extract
 326 more useful information, we introduced a learnable reference set to encode nodes into a latent
 327 expressive probability space. Compared with the deterministic way, BernPool possessed more
 328 diversity to capture salient substructures. Then, to jointly learn representative substructures and
 329 preserve graph topology information, we proposed a hybrid graph pooling paradigm that fuses two
 330 pooling manners. We evaluate BernPool on multiple widely used datasets and dissected the framework
 331 with ablation analysis. The experimental results show that BernPool outperforms state-of-the-art
 332 methods and demonstrates the effectiveness of our proposed modules.

333 References

- 334 [1] Filippo Maria Bianchi, Daniele Grattarola, and Cesare Alippi. Spectral clustering with graph
335 neural networks for graph pooling. In *International conference on machine learning*, pages
336 874–883. PMLR, 2020.
- 337 [2] Karsten M Borgwardt, Cheng Soon Ong, Stefan Schönauer, SVN Vishwanathan, Alex J
338 Smola, and Hans-Peter Kriegel. Protein function prediction via graph kernels. *Bioinformatics*,
339 21(suppl_1):i47–i56, 2005.
- 340 [3] Frederik Diehl. Edge contraction pooling for graph neural networks. *arXiv preprint*
341 *arXiv:1905.10990*, 2019.
- 342 [4] Paul D Dobson and Andrew J Doig. Distinguishing enzyme structures from non-enzymes
343 without alignments. *Journal of molecular biology*, 330(4):771–783, 2003.
- 344 [5] David K Duvenaud, Dougal Maclaurin, Jorge Iparraguirre, Rafael Bombarell, Timothy Hirzel,
345 Alán Aspuru-Guzik, and Ryan P Adams. Convolutional networks on graphs for learning
346 molecular fingerprints. *Advances in neural information processing systems*, 28, 2015.
- 347 [6] David K Duvenaud, Dougal Maclaurin, Jorge Iparraguirre, Rafael Bombarell, Timothy Hirzel,
348 Alan Aspuru-Guzik, and Ryan P Adams. Convolutional networks on graphs for learning
349 molecular fingerprints. In C. Cortes, N. Lawrence, D. Lee, M. Sugiyama, and R. Garnett,
350 editors, *Advances in Neural Information Processing Systems*, volume 28. Curran Associates,
351 Inc., 2015.
- 352 [7] Wenzheng Feng, Jie Zhang, Yuxiao Dong, Yu Han, Huanbo Luan, Qian Xu, Qiang Yang,
353 Evgeny Kharlamov, and Jie Tang. Graph random neural networks for semi-supervised learning
354 on graphs. *Advances in neural information processing systems*, 33:22092–22103, 2020.
- 355 [8] Aasa Feragen, Niklas Kasenburg, Jens Petersen, Marleen de Bruijne, and Karsten Borgwardt.
356 Scalable kernels for graphs with continuous attributes. *Advances in neural information process-*
357 *ing systems*, 26, 2013.
- 358 [9] Matthias Fey and Jan Eric Lenssen. Fast graph representation learning with pytorch geometric.
359 *arXiv preprint arXiv:1903.02428*, 2019.
- 360 [10] Hongyang Gao and Shuiwang Ji. Graph u-nets. In *international conference on machine learning*,
361 pages 2083–2092. PMLR, 2019.
- 362 [11] Xing Gao, Wenrui Dai, Chenglin Li, Hongkai Xiong, and Pascal Frossard. ipool—information-
363 based pooling in hierarchical graph neural networks. *IEEE Transactions on Neural Networks*
364 *and Learning Systems*, 33(9):5032–5044, 2021.
- 365 [12] M. Gori, G. Monfardini, and F. Scarselli. A new model for learning in graph domains. In
366 *Proceedings. 2005 IEEE International Joint Conference on Neural Networks, 2005.*, volume 2,
367 pages 729–734 vol. 2, 2005.
- 368 [13] Will Hamilton, Zhitaoy Ying, and Jure Leskovec. Inductive representation learning on large
369 graphs. *Advances in neural information processing systems*, 30, 2017.
- 370 [14] Takeshi D Itoh, Takatomi Kubo, and Kazushi Ikeda. Multi-level attention pooling for graph
371 neural networks: Unifying graph representations with multiple localities. *Neural Networks*,
372 145:356–373, 2022.
- 373 [15] Jeroen Kazius, Ross McGuire, and Roberta Bursi. Derivation and validation of toxicophores for
374 mutagenicity prediction. *Journal of medicinal chemistry*, 48(1):312–320, 2005.
- 375 [16] Thomas N Kipf and Max Welling. Semi-supervised classification with graph convolutional
376 networks. *arXiv preprint arXiv:1609.02907*, 2016.
- 377 [17] Junhyun Lee, Inyeop Lee, and Jaewoo Kang. Self-attention graph pooling. In *International*
378 *conference on machine learning*, pages 3734–3743. PMLR, 2019.

- 379 [18] Maosen Li, Siheng Chen, Ya Zhang, and Ivor Tsang. Graph cross networks with vertex infomax
380 pooling. *Advances in Neural Information Processing Systems*, 33:14093–14105, 2020.
- 381 [19] David Liben-Nowell and Jon Kleinberg. The link prediction problem for social networks. In
382 *Proceedings of the twelfth international conference on Information and knowledge management*,
383 pages 556–559, 2003.
- 384 [20] Yunsheng Pang, Yunxiang Zhao, and Dongsheng Li. Graph pooling via coarsened graph
385 infomax. In *Proceedings of the 44th International ACM SIGIR Conference on Research and*
386 *Development in Information Retrieval*, pages 2177–2181, 2021.
- 387 [21] Pál András Papp, Karolis Martinkus, Lukas Faber, and Roger Wattenhofer. Dropgnn: Random
388 dropouts increase the expressiveness of graph neural networks. *Advances in Neural Information*
389 *Processing Systems*, 34:21997–22009, 2021.
- 390 [22] Ekagra Ranjan, Soumya Sanyal, and Partha Talukdar. Asap: Adaptive structure aware pooling
391 for learning hierarchical graph representations. In *Proceedings of the AAAI Conference on*
392 *Artificial Intelligence*, volume 34, pages 5470–5477, 2020.
- 393 [23] Franco Scarselli, Marco Gori, Ah Chung Tsoi, Markus Hagenbuchner, and Gabriele Monfardini.
394 The graph neural network model. *IEEE Transactions on Neural Networks*, 20(1):61–80, 2009.
- 395 [24] Nino Shervashidze, Pascal Schweitzer, Erik Jan Van Leeuwen, Kurt Mehlhorn, and Karsten M
396 Borgwardt. Weisfeiler-lehman graph kernels. *Journal of Machine Learning Research*, 12(9),
397 2011.
- 398 [25] Petar Velickovic, Guillem Cucurull, Arantxa Casanova, Adriana Romero, Pietro Lio, Yoshua
399 Bengio, et al. Graph attention networks. *stat*, 1050(20):10–48550, 2017.
- 400 [26] Oriol Vinyals, Samy Bengio, and Manjunath Kudlur. Order matters: Sequence to sequence for
401 sets. *arXiv preprint arXiv:1511.06391*, 2015.
- 402 [27] Zhengyang Wang and Shuiwang Ji. Second-order pooling for graph neural networks. *IEEE*
403 *Transactions on Pattern Analysis and Machine Intelligence*, 2020.
- 404 [28] Lanning Wei, Huan Zhao, Quanming Yao, and Zhiqiang He. Pooling architecture search for
405 graph classification. In *Proceedings of the 30th ACM International Conference on Information*
406 *& Knowledge Management*, pages 2091–2100, 2021.
- 407 [29] Junran Wu, Xueyuan Chen, Ke Xu, and Shangzhe Li. Structural entropy guided graph hierarchi-
408 cal pooling. In *International Conference on Machine Learning*, pages 24017–24030. PMLR,
409 2022.
- 410 [30] Keyulu Xu, Weihua Hu, Jure Leskovec, and Stefanie Jegelka. How powerful are graph neural
411 networks? *arXiv preprint arXiv:1810.00826*, 2018.
- 412 [31] Pinar Yanardag and SVN Vishwanathan. Deep graph kernels. In *Proceedings of the 21th ACM*
413 *SIGKDD international conference on knowledge discovery and data mining*, pages 1365–1374,
414 2015.
- 415 [32] Pinar Yanardag and SVN Vishwanathan. A structural smoothing framework for robust graph
416 comparison. *Advances in neural information processing systems*, 28, 2015.
- 417 [33] Zhitao Ying, Jiaxuan You, Christopher Morris, Xiang Ren, Will Hamilton, and Jure Leskovec.
418 Hierarchical graph representation learning with differentiable pooling. *Advances in neural*
419 *information processing systems*, 31, 2018.
- 420 [34] Hao Yuan and Shuiwang Ji. Structpool: Structured graph pooling via conditional random fields.
421 In *Proceedings of the 8th International Conference on Learning Representations*, 2020.
- 422 [35] Muhan Zhang and Yixin Chen. Link prediction based on graph neural networks. *Advances in*
423 *neural information processing systems*, 31, 2018.

- 424 [36] Muhan Zhang, Zhicheng Cui, Marion Neumann, and Yixin Chen. An end-to-end deep learning
425 architecture for graph classification. In *Proceedings of the AAAI conference on artificial*
426 *intelligence*, volume 32, 2018.
- 427 [37] Zhen Zhang, Jiajun Bu, Martin Ester, Jianfeng Zhang, Zhao Li, Chengwei Yao, Huifen Dai,
428 Zhi Yu, and Can Wang. Hierarchical multi-view graph pooling with structure learning. *IEEE*
429 *Transactions on Knowledge and Data Engineering*, 35(1):545–559, 2021.